Direct temperature monitoring for semiconductors in plasma immersion ion implantation

Xiubo Tian and Paul K. Chu[a)]
Department of Physics and Materials Science, City University of Hong Kong, Kowloon, Hong Kong

(Received 28 January 2000; accepted for publication 9 March 2000)

In situ temperature monitoring is extremely important in plasma immersion ion implantation (PIII) of semiconductors. For instance, the silicon wafer must be heated to 600 °C or higher in separation by plasma implantation of oxygen, and in the PIII/ion-cut process, the wafer temperature must remain below 300 °C throughout the experiment. In this article, we present a thermocouple-based direct temperature measurement system for planar samples such as silicon wafers. In order to ensure reliable high-voltage operation and overall electrical isolation, the thermocouple assembly and wires are integrated into the sample chuck and feedthrough. Hydrogen plasma immersion ion implantation is performed in silicon to demonstrate the effectiveness and reliability of the device. Our experimental results indicate that instrumental parameters such as implantation voltage, pulse duration, and pulsing frequency affect the sample temperature to a different extent. The measured temperature rise is higher than that predicted by a theoretical model based on the Child–Langmuir law. The discrepancy is attributed to the finite-sample size and the nonplanar, conformal plasma sheath. © *2000 American Institute of Physics.* [S0034-6748(00)02307-8]

I. INTRODUCTION

Ion implantation is an effective surface modification and processing technique for semiconductors, polymers, and metals.[1] An alternative method, plasma immersion ion implantation (PIII),[2–5] has recently emerged and is superior to conventional beam-line ion implantation in several aspects such as sample throughput and equipment cost. In addition, PIII circumvents the line-of-sight and retained-dose limitations inherent to conventional beam-line ion implantation. In many semiconductor PIII applications, the effectiveness of the process hinges on precise control of the substrate temperature in addition to the implantation voltage and ion dose. Accurate and reliable *in situ* temperature monitoring in separation by plasma implantation of oxygen (SPIMOX),[6–9] hydrogen PIII/ion cut,[10–12] and elevated-temperature PIII,[13–16] is crucial to the success. For example, the silicon wafer temperature must be kept at 600 °C or higher in SPIMOX, whereas in the hydrogen PIII/ion-cut process, the wafer temperature must remain below 300 °C during implantation.

For conventional beam-line ion implantation, temperature monitoring or calculation is much easier on account of the low sample potential (usually at ground). In contrast, for PIII, the high sample voltage and secondary electrons galore impose a big hurdle for direct temperature measurement. Hence, remote temperature sensing techniques using pyrometers have been more common in PIII and they are generally quite safe to use.[17] However, in many practical semiconductor applications, this technique has several drawbacks, such as limited temperature range (multiple pyrometers needed for a wide temperature range), interference due to electromagnetic field and plasma, as well as difficulty to measure multiple points on the wafer. In addition, natural degradation and contamination of the quartz windows between the pyrometer and sample by the plasma can introduce errors to the temperature measurement. We have developed a simple *in situ* temperature monitoring system using a thermocouple, and it has been demonstrated to work effectively at low implantation voltage (less than 20 kV).[18] Our initial success and the need for a high-voltage temperature measurement device for SPIMOX and ion cut have prompted us to design a more versatile and robust system that can measure a wide temperature range at voltages above 50 kV.

II. HARDWARE

The semiconductor PIII instrument in City University of Hong Kong comprises a vacuum chamber 1000 mm in height and 750 mm in diameter, a radio-frequency (rf) inductively coupled plasma source, and a 100 kV, 300 A solid-state power modulator. Air-cooling and resistive-heating mechanisms are implemented on the sample holder to allow for elevated temperature experiments such as SPIMOX or low- (room-) temperature PIII work such as hydrogen PIII/ion cut. The target feedthrough is hollow to allow cooled, compressed air to circulate to the sample chuck and the room makes it possible to integrate our temperature sensing device into the sample stage. Figure 1 displays the schematic of the temperature monitoring system that is different from, and also a big improvement over, the one reported by us earlier.[18] The thermocouple head is screwed into the target platen about 3 mm away from the top surface. Multiple thermocouples can be installed if temperature information on multiple locations is required. Unlike the old design, the connecting wires are placed inside the stainless-steel tube beneath the center of the target platen. On the upper part of the tube, a hole 3 mm in diameter is drilled for pumping. *F*

[a)]Author to whom correspondence should be addressed; electronic mail: paul.chu@cityu.edu.hk

 © 2000 American Institute of Physics

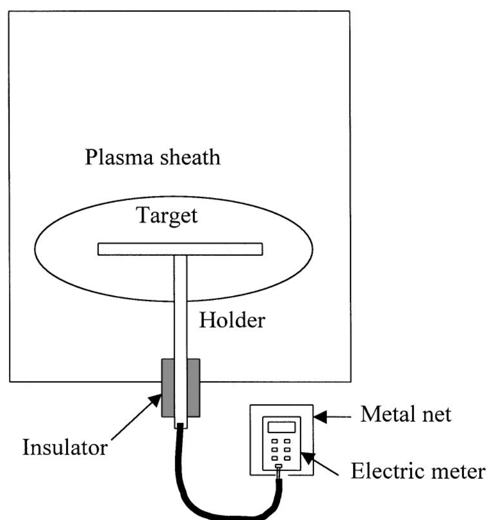

FIG. 1. Schematic of the *in situ* temperature measurement system in the plasma immersion ion implanter.

rubber is used to seal the insulator and tube. The display meter is placed outside of the instrument and covered by a metal net. One of the wires transmitting the temperature information is connected to the net. This is very critical to stable and reliable measurements. Arcing or sparking frequently takes place during PIII, especially under high voltage, and induces a sudden change in the potential difference between the target and earth (anode). The meter is subjected to the same dynamic process, and if the potential difference on the meter is more than 60 V, the meter can be damaged. In our setup, the thermocouple wire contacts the shielding net surrounding the meter. Both components have the same instantaneous potential no matter how the target voltage and electromagnetic field vary. As shown in Fig. 2, the shielded meter is located on an insulated capacitance divider. By positioning and isolating the wires inside the sample feedthrough carefully, our device functions very well even at high potential (over 50 kV) and under severe arcing conditions. This is a big improvement over our old system that only works below 20 kV.

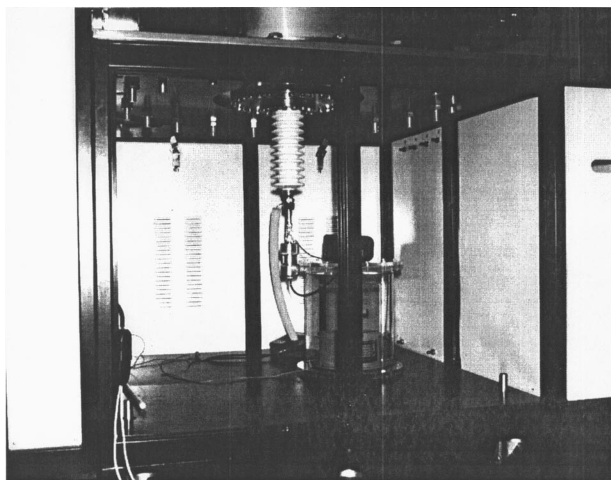

FIG. 2. Photograph of the high-voltage feedthrough underneath the PIII vacuum chamber and the meter (black object above the cylindrical oil container).

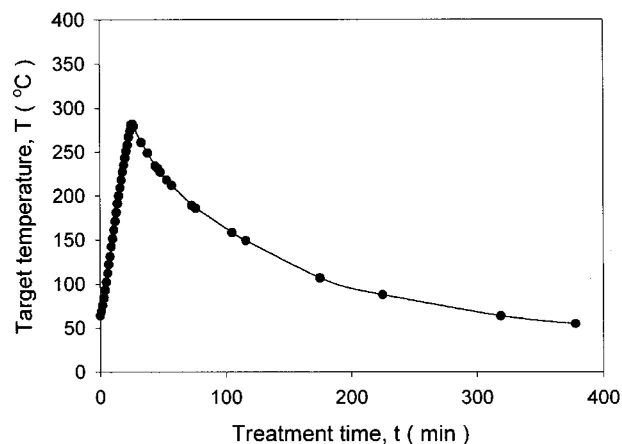

FIG. 3. Temperature variation during and after hydrogen PIII (pulse duration=30 μs).

III. EXPERIMENT

A. Heating and cooling mechanisms

With our new temperature monitoring device, we can investigate the heating and cooling processes in PIII in much more detail than before. Our initial control experiments with/without high voltage and with/without plasma demonstrate that the negative potential and plasma have almost no influence on the measurement results. Our previous results show that during PIII, the sample is heated mainly by the energetic ions accelerated by the plasma sheath and cooled naturally by conduction and radiation.[18] Figure 3 shows the measured temperature change in a PIII experiment using an implantation voltage of 30 kV, pulsing frequency of 330 Hz, pulse duration of 30 μs, hydrogen plasma density of 1.0×10^9 ions/cm^3, and working pressure of 3.6×10^{-4} Torr. Our results confirm that heating from the plasma without ion bombardment is very little. The temperature ramp rate is about 0.1 °C/min without ion bombardment compared to 10 °C/min with implantation.

According to Fig. 3, the temperature rise is almost linearly proportional to the implantation time during the entire voltage pulse, implying that the net heating power is nearly constant. This is theoretically possible since cooling is determined by heat conduction through the holder and stainless-steel tube feedthrough, and to a lesser extent radiation loss. Both of these two heat loss mechanisms have only a minor effect. The tube wall is relatively thin and there are only three direct contacting points to the target platen, and so heat loss by conduction is small. Cooling by thermal radiation is also small when the sample temperature is low, like in the temperature range shown in Fig. 3 since the radiation heat loss is proportional to T^4. After the voltage pulse is turned off, the sample temperature begins to decrease after a small time delay from thermal inertia. The fall is basically consistent with an exponential decay characteristic of radiation cooling. At a higher temperature, the cooling rate is higher, for instance, -3 °C/min at 270 °C vs -0.82 °C/min at 150 °C. Hence, the rate of heat loss without ion-beam bombardment (even at 270 °C) is much slower than that of the temperature rise with the voltage pulse on. The overall result is that ion-beam-induced heating is the dominant phenom-

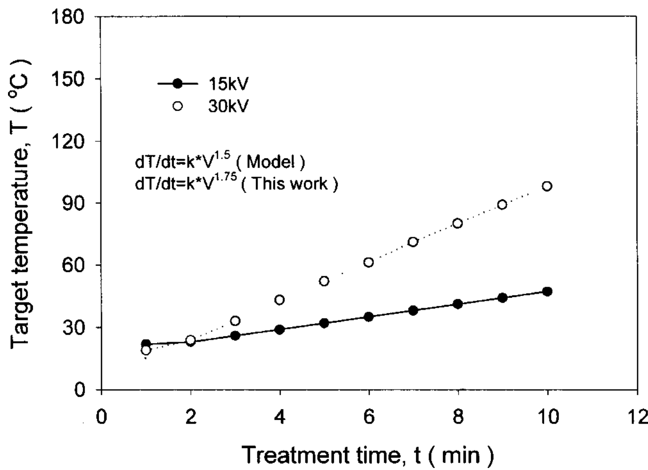

FIG. 4. Sample temperature rise at two implantation voltages.

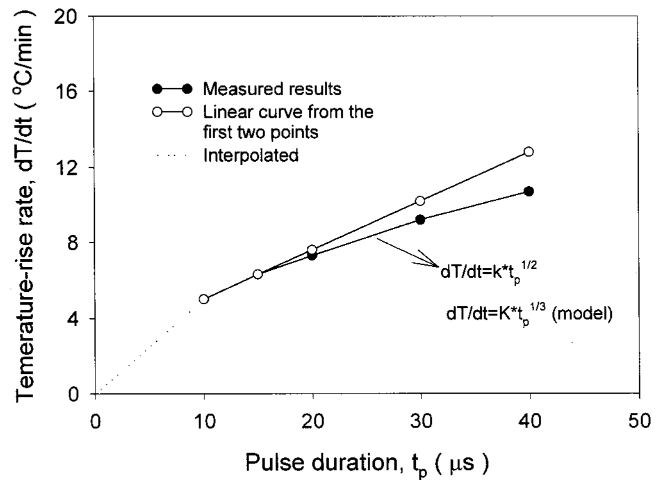

FIG. 5. Relationship of sample temperature vs pulse duration. The upper (empty circle) curve is extrapolated from the first two data points (10 and 15 μs), whereas the dotted line between 0 and 10 μs is an artificial interpolation.

enon while heat loss in this temperature range is insignificant, thereby leading to the observed linear increase in sample temperature, even though the relationship is not expected to be linear at higher temperature due to higher heat loss. From the cooling behavior, it can be deduced that the equilibrium temperature will reach about 500 °C if the pulse width is increased.

B. Influence of temperature rise by implantation voltage, pulse duration, and frequency

1. Implantation voltage

As shown in Fig. 4, the implantation voltage affects the ion heating power significantly and nonlinearly. At a constant pulse duration and frequency (30 μs and 330 Hz), the rate of temperature rise is 3 °C/min when the implantation voltage is 15 kV compared to 9.5 °C/min at 30 kV. A factor of 2 increase in the implantation voltage gives rise to a factor of 3 increase in the temperature ramp rate. At 30 kV, the sample will reach 300 °C within 30 min. This is the upper limit of the hydrogen PIII/ion cut, otherwise premature surface blistering will occur. That is to say, the implantation process must end before 30 min if the above parameters are used, or the pulse duration or frequency must be reduced. The latter processes will increase the implantation time, making PIII less attractive compared to beam-line ion implantation. If shorter time is needed to increase throughput, the plasma density, pulse width, and/or pulsing frequency must be increased, but an efficient sample cooling device must be installed.

2. Pulse duration

Figure 5 demonstrates the effect of the pulse duration on the sample temperature rise. Although the temperature increases when the pulse duration is longer, the relationship is nonlinear but different from that with the implantation voltage. When the pulse width is small, the temperature rise is more sensitive to the pulse duration variation. The rate of temperature increase is progressively smaller at longer pulse width, as indicated by an extrapolation of the first two data points (10 and 15 μs). The dotted line between 0 and 10 μs is an artificial interpolation just to illustrate that the rate of temperature rise in this range is even higher.

3. Pulsing frequency

Contrary to the temperature rise with respect to implantation voltage and pulse duration, the relationship between the temperature rise and pulsing frequency is almost linear, as shown in Fig. 6. At 100 Hz, the rate of temperature rise is 2.9 °C/min, compared to 5.8 °C/min at 200 Hz and 9.5 °C/min at 330 Hz. Our results also indicate that it is much easier to control the sample temperature rise by varying the pulsing frequency than the pulse duration.

IV. DISCUSSION

From the above experimental results, the three main implantation parameters: implantation voltage, pulse duration, and pulsing frequency, have different effects on the sample temperature and temperature rise. Assuming that sample heating results primarily from energetic ion bombardment and that all the ions in the sheath are implanted into the

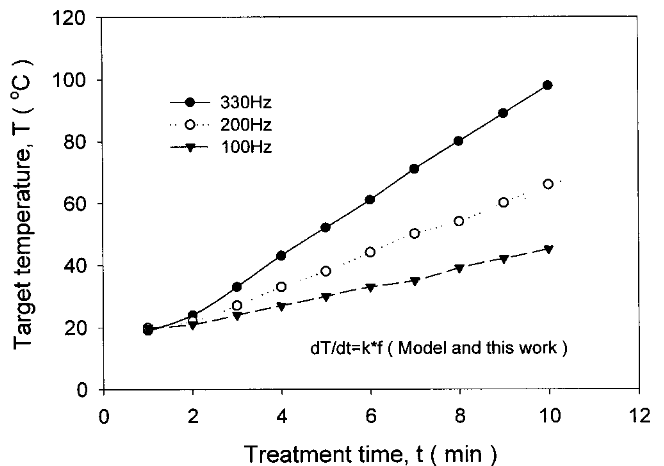

FIG. 6. Sample temperature rise for different pulsing frequencies.

surface with energy of eV_0, the heating power can be derived from the Child–Langmuir law.[19–21] The sheath thickness S_t, is calculated by[22]

$$S_t = S_0(\tfrac{2}{3}\omega_{\mathrm{pi}} + 1)^{1/3}, \tag{1}$$

where ω_{pi} is the ion plasma frequency and S_0 is the ion-matrix sheath thickness. Thus the energy W deposited into a unit area by the ions in a single pulse is

$$W = n_i S_t e V_0, \tag{2}$$

where n_i is the plasma density. The average ion heating power P_{ave} is

$$P_{\mathrm{ave}} = fW, \tag{3}$$

where f is the pulsing frequency.

If we ignore the instantaneous dynamic ion heating process for simplicity,[23] the deposited energy can be calculated by the sheath width at the end of the pulse, t_p. Thus,

$$P_{\mathrm{ave}} = f n_i^{0.5} V_0^{1.5} (2e\epsilon_0)^{0.5} \left[\frac{2}{3} \left(\frac{n_i e^2}{\epsilon_0 M} \right)^{0.5} t_p + 1 \right]^{1/3}, \tag{4}$$

where e is the ion charge, ϵ_0 is the free-space permittivity, and M is the ion mass. For a typical set of implantation parameters, e.g., $n_i = 1.0 \times 10^{15}/\mathrm{m}^3$, H_2^+ plasma, $t_p \geqslant 10\ \mu\mathrm{s}$, $\frac{2}{3}(ne^2/\epsilon_0 M)^{0.5} t_p \gg 1$, Eq. (4) can be simplified to be

$$P_{\mathrm{ave}} = (\tfrac{2}{3})^{1/3} 2^{1/2} e^{5/6} \epsilon_0^{1/3} t_p^{1/3} M^{-1/6} f V_0^{1.5} n^{2/3}. \tag{5}$$

By considering the exponent of each term, the implantation voltage (V_0) has the largest impact on the temperature rise. When the implantation voltage is increased, the implanted ions will have higher energy. At the same time, the sheath expansion is also accelerated, leading to more energetic ions implanted into the target in a single pulse. Hence, the sample receives more heat at a higher implantation voltage. With regard to the pulse duration, a longer pulse width produces a thicker plasma sheath also giving rise to more implanted ions. However, the sheath expansion obeys the Child–Langmuir law stating that the sheath expansion becomes slower as time elapses. Therefore, the temperature rise due to increasing pulse width is not as much as that from raising the sample voltage. Our experimental results described in Sec. III are more or less in line with the theoretical prediction, although two exponents are a little higher than those in Eq. (5). The experimentally determined exponent of the implantation voltage (V_0) is about 1.75 compared to the theoretical value of 1.5, and that of the pulse duration (t) is about 1/2 in contrast to 1/3 in the equation. The minor discrepancy can be attributed to the fact that the derivation of Eq. (5) assumes a planar plasma sheath. In our experiments and reality, the plasma sheath is planar only close to the center of the sample and gradually assumes a dome or mushroom shape as time elapses due to the finite size of the sample as well as the sample stage. Consequently, more ions are implanted into the sample than in the ideal infinitely large planar target case.

In summary, we have designed and constructed a new *in situ* temperature measurement device for plasma immersion ion implantation. The thermocouple and connecting wires are integrated into the sample chuck to provide better isolation from the plasma environment. The device has been tested to function reliably at voltages exceeding 50 kV. Using this direct temperature monitoring device, the heating and cooling phenomena during PIII, and the influence of the sample temperature by the sample, high voltage, pulse width, as well as pulsing frequency are investigated. The sample temperature is more sensitive to implantation voltage variation, whereas the rate of temperature change is linear versus pulsing frequency. Our experimental results also indicate that the ion heating power derived from the Child–Langmuir law by assuming ion bombardment to be the main heating mechanism and a planar sheath underestimates the effects of the implantation voltage and pulse width. The discrepancy can be explained by the nonplanar and conformal plasma sheath for a finite-size sample.

ACKNOWLEDGMENTS

The work was supported by Hong Kong Research Grants Council earmarked Grant Nos. 9040344 and 9040412 as well as Hong Kong RGC Germany Joint Scheme Nos. 9050084 and 9050150.

[1] J. S. Williams, R. G. Elliman, and M. C. Ridgway, *Ion Beam Modification of Metals* (North-Holland, Elsevier Science, Amsterdam, 1996).

[2] J. R. Conrad, J. L. Radtke, R. A. Dodd, F. J. Worzala, and N. C. Tran, J. Appl. Phys. **2**, 4951 (1987).

[3] J. Tendys, I. J. Donnelly, M. J. Kenny, and J. T. A. Pollock, Appl. Phys. Lett. **53**, 2143 (1988).

[4] S. Mandl, N. P. Barradas, J. Brutsher, R. Grunzel, and W. Moller, Nucl. Instrum. Methods Phys. Res. B **127/128**, 996 (1997).

[5] P. K. Chu, S. Qin, C. Chan, N. W. Cheung, and P. K. Ko, IEEE Trans. Plasma Sci. **26**, 79 (1998).

[6] J. Min, P. K. Chu, Y. C. Cheng, J. B. Liu, S. Im, S. Iyer, and N. M. Cheung, Mater. Chem. Phys. **40**, 219 (1995).

[7] P. K. Chu, N. W. Cheung, and C. Chan, Semicond. Int. **6**, 165 (1996).

[8] J. Min, P. K. Chu, Y. C. Cheng, J. Liu, S. S. Iyer, and N. W. Cheung, Surf. Coat. Technol. **85**, 60 (1996).

[9] J. B. Liu, S. Iyer, C. M. Hu, N. W. Cheung, R. Gronsky, J. Min, and P. Chu, Appl. Phys. Lett. **67**, 2361 (1995).

[10] Z. Fan, P. K. Chu, C. Chan, and N. W. Cheung, Appl. Phys. Lett. **73**, 202 (1998).

[11] P. K. Chu, X. Lu, S. S. K. Iyer, and N. W. Cheung, Solid State Technol. **40**, S9 (1997).

[12] X. Liu, N. W. Cheung, M. D. Strathman, P. K. Chu, and B. Doyle, Appl. Phys. Lett. **71**, 1804 (1997).

[13] C. Blawert, B. L. Mordike, G. A. Collins, K. T. Short, and J. Tendys, Surf. Coat. Technol. **103/104**, 240 (1998).

[14] G. A. Collins, R. Hutchings, K. T. Short, J. Tendys, X. Li, and M. Samandi, Surf. Coat. Technol. **74**, 417 (1995).

[15] X. B. Tian, X. F. Wang, B. Y. Tang, P. K. Chu, P. K. Ko, and Y. C. Cheng, Rev. Sci. Instrum. **70**, 1824 (1999).

[16] X. B. Tian, Z. M. Zeng, T. Zhang, B. Y. Tang, and P. K. Chu, Thin Solid Films **366**, 150 (2000).

[17] G. A. Collins, R. Hutchings, K. T. Short, J. Tendys, and C. H. Van der Valk, Surf. Coat. Technol. **84**, 537 (1996).

[18] X. B. Tian, Z. N. Fan, X. C. Zeng, Z. M. Zeng, B. Y. Tang, and P. K. Chu, Rev. Sci. Instrum. **70**, 2818 (1999).

[19] M. Lieberman, J. Appl. Phys. **66**, 2926 (1989).

[20] J. T. Scheuder, M. Shamim, and J. R. Conrad, J. Appl. Phys. **67**, 1241 (1990).

[21] S. Qin and C. Chan, IEEE Trans. Plasma Sci. **20**, 569 (1992).

[22] P. K. Chu, S. Qin, C. Chan, N. W. Cheung, and L. A. Larson, Mater. Sci. Eng. Rep. **R17**, 207 (1996).

[23] J. P. Blanchard, J. Vac. Sci. Technol. B **12**, 910 (1994).